

Spin Dependence of the Electron Mean Free Path in Fe, Co, and Ni

R. W. Rendell and David R. Penn

National Bureau of Standards, Washington, D. C. 20234

(Received 2 September 1980)

Spin-dependent electron mean free paths as a function of the hot electron energy are calculated for Fe, Co, and Ni. The difference in mean free paths of electrons for spin parallel and antiparallel to the majority spin direction of the ferromagnet is found to change sign and decrease rapidly in magnitude with increasing electron energy. Results for the mean free path with and without exchange included are also presented.

PACS numbers: 71.45.Gm, 72.15.Lh

The mean free path (MFP) of hot electrons in a ferromagnetic material may be spin dependent because the majority-spin-electron density differs from the minority-spin-electron density and only electrons of parallel spin undergo an exchange interaction. It has been pointed out by DeWames and Vredevoe¹ and more recently by Bringer *et al.*² that the spin dependence of the electron MFP may be an important factor in the interpretation of photoemission experiments which measure the spin polarization of the photoexcited electrons. Bringer *et al.*² and Feder³ assumed that an electron can only interact with an electron of opposite spin at low energy because of the cancellation of the direct Coulomb interaction by the exchange term with consequence that $\lambda^\uparrow/\lambda^\downarrow = n^\uparrow/n^\downarrow$, where n^\uparrow (n^\downarrow) is the number of majority- (minority-) spin electrons in the solid and λ^\uparrow (λ^\downarrow) is the MFP for electrons with spin parallel (antiparallel) to the majority-spin direction. Our purpose is to give a more accurate estimate of the spin dependence of the electron MFP as a function of electron kinetic energy in Fe, Co, and Ni as well as to report calculations of the MFP with and without exchange for free-electron-like materials as well as for Fe, Co, and Ni. We find that the work of Bringer *et al.*² and Feder³ greatly overestimates the MFP asymmetry, given by $A = (\lambda^\downarrow - \lambda^\uparrow)/(\lambda^\downarrow + \lambda^\uparrow)$, and, in fact, it usually gives the wrong sign for this quantity. Furthermore, our calculations neglect correlation effects which reduce $|A|$ still further. The results of the present calculation, based on the statistical and Born approximation described below, imply that the spin dependence of the MFP cannot explain the anomalously high values of the spin polarization of the photoyield measured by Bringer *et al.*² and, in fact, similar experiments on Co do not produce an anomalous result.⁴

In addition, the elastic scattering of polarized electrons from a Ni surface has been measured in a very elegant experiment by Celotta *et al.*,⁵

who observed an asymmetry in the scattered electrons. The most appealing interpretation of their results is that the asymmetry results from the exchange interaction between the scattered electrons and those of Ni. However, it could also result from the spin dependence of the electron MFP; electrons entering the solid can be scattered inelastically and the resulting asymmetry in the elastic scattering is proportional to A . From the small magnitude we calculate for A in Ni it can be concluded that the results of the polarized electron scattering from Ni obtained by Celotta *et al.*⁵ cannot be explained by a spin-dependent MFP with the consequence that their experiment may well be a direct measure of the magnetic exchange scattering at the Ni surface.

Our calculations of the spin-dependent MFP for Fe, Co, and Ni are based on the statistical approximation introduced by Lindhard and co-workers⁶ who calculated the energy loss of charged particles in a variety of materials. It has subsequently been used by a number of authors to calculate the stopping power for protons, ions, electrons, and α particles in a number of solids. It has recently been employed by Tung, Ashley, and Ritchie⁷ to calculate the electron MFP for Al, Si, Ni, Cu, Ag, and Au with very good results. The statistical approximation bears some resemblance to the local density approximation; the electrons in a volume element of the metal are characterized by a local density and the contribution of those electrons to the scattering of a hot electron [i.e., to $\lambda^{-1}(\vec{r})$] is taken to be that of a free-electron gas of the same density, λ_F^{-1} . The total inverse MFP is obtained by integrating λ_F^{-1} over the Wigner-Seitz cell of the metal.

The effects of exchange and correlation on the electron-electron interaction in a free-electron gas have been studied in much detail; however, the treatment has not been extended to include dynamic screening as is required for the treatment of electron energy loss and MFP calcula-

tion.⁶ Therefore, we have used the fact that the electron-electron interaction between parallel spin electrons must be antisymmetric with respect to the electron coordinates. We choose the interaction between antiparallel-spin electrons to be the Coulomb interaction screened by the Lindhard dielectric function and that between parallel-spin electrons to be the antisymmetrized screened (Lindhard) Coulomb interaction. This represents an extension of the work of Ritchie

and Ashley,⁸ who calculated the effects of exchange on the MFP of low-energy electrons in a free-electron gas; for energies $\epsilon \lesssim 1.1\epsilon_F$ (ϵ_F is the Fermi energy) dynamic screening can be neglected.

Let a hot electron with momentum \vec{p}_0 , energy ϵ_{p_0} and spin σ interact with an electron from the solid and scatter into the final state $\vec{p}_f, \epsilon_{p_f}, \sigma$. The electron from the solid scatters from $\vec{l}_0, \epsilon_{l_0}, \sigma'$ to $\vec{l}_f, \epsilon_{l_f}, \sigma'$. The scattering rate for this event in the Born approximation is given by

$$P^\sigma(p_0) = \frac{2\pi}{\hbar} \sum_{i_0, i_f, p_f, \sigma'} (1 - f_{p_f \sigma})(1 - f_{i_f \sigma'}) f_{i_0 \sigma'} |U(|\vec{p}_0 - \vec{p}_f|, \epsilon_{p_0} - \epsilon_{p_f}) - \delta_{\sigma\sigma'} U(|\vec{p}_0 - \vec{l}_f|, \epsilon_{p_0} - \epsilon_{i_f})|^2 \times \delta(\vec{p}_0 + \vec{l}_0 - \vec{p}_f - \vec{l}_f) \delta(\epsilon_{p_0} + \epsilon_{i_0} - \epsilon_{p_f} - \epsilon_{i_f}), \quad (1)$$

where $U(q, \omega)$ is the dynamically screened electron-electron interaction and f is a Fermi function. We use Eq. (1) to study the free-electron case by taking $U(q, \omega) = v_q / \epsilon(q, \omega)$ where the Coulomb potential v_q is screened by the Lindhard dielectric function⁹ $\epsilon(q, \omega)$, which neglects exchange and correlation. Thus the effects of exchange are taken into account through the antisymmetrization in Eq. (1). The Born approximation for a dynamically screened potential has not been rigorously justified at these low energies; however, the velocity of the hot electron relative to an electron in the metal must always be greater or on the order of the Fermi velocity. Lindhard⁹ has argued that the strongly screened Coulomb field can be considered small in the sense of perturbation theory.

The interaction in Eq. (1) is antisymmetric in the electron coordinates in the case where the incident hot-electron spin is parallel to the spin of the interacting electron in the solid ($\sigma' = \sigma$). The contribution to Eq. (1) when the spins are antiparallel ($\sigma' = \bar{\sigma}$) can be written as

$$P_D^{\sigma\bar{\sigma}}(p_0) = \frac{a_0^{-1}}{2\pi} \frac{2\epsilon_F}{\hbar p_0} \int_0^{x_m} dx_1 \int \frac{dz_1}{z_1} \text{Im} \left(\frac{-1}{\epsilon(x_1, z_1)} \right), \quad (2)$$

where $x_1 = (\epsilon_{p_0} - \epsilon_{p_f}) / \epsilon_F$, $x_m = (\epsilon_{p_0} - \epsilon_F) / \epsilon_F$, $z_1 = |\vec{p}_0 - \vec{p}_f| / 2k_F$, and a_0 is the Bohr radius. Equation (2) measures the scattering into electron-hole pairs and plasmons without exchange scattering, and was originally derived by Quinn and Ferrell.¹⁰ When the spins are parallel the contribution to Eq. (1) from the interference between direct and exchange scattering can be written as

$$P_I^{\sigma\sigma}(p_0) = \frac{a_0^{-1}}{(2\pi)^2} \frac{\hbar}{2ma_0} \frac{\epsilon_F}{\epsilon_{p_0}} \int dx_1 \int dx_2 \int \frac{dz_1}{z_1^2} \int \frac{dz_2}{z_2^2} g(x_1, z_1; x_2, z_2), \quad (3)$$

where

$$g(x_1, z_1; x_2, z_2) = \left[\text{Im} \left(\frac{-1}{\epsilon(x_1, z_1)} \right) \text{Im} \left(\frac{-1}{\epsilon(x_2, z_2)} \right) + \text{Re} \left(\frac{-1}{\epsilon(x_1, z_1)} \right) \text{Re} \left(\frac{-1}{\epsilon(x_2, z_2)} \right) \right] [1 - \alpha^2(x_1, z_1) - \alpha^2(x_2, z_2)]^{-1/2} \quad (4)$$

and

$$\alpha(x, z) = (x + 4z^2) [4(p_0/k_f)z]^{-1}. \quad (5)$$

The exchange-scattering process provides the extra momentum and energy transfer, $x_2 = (\epsilon_{p_0} - \epsilon_{i_f}) / \epsilon_F$ and $z_2 = |\vec{p}_0 - \vec{l}_f| / 2k_F$, in this expression. Momentum and energy conservation impose restrictions on the integrations in Eq. (3).

Parallel-spin scattering also contributes a term $P_D^{\sigma\sigma}(p_0)$ identical to Eq. (2) and the total scattering rate can be written

$$P^\sigma(p_0) = [P_D^{\sigma\sigma}(p_0) + P_D^{\sigma\bar{\sigma}}(p_0)] - P_I^{\sigma\sigma}(p_0), \quad (6)$$

where $P_D^{\sigma\sigma}(p_0) = P_D^{\sigma\bar{\sigma}}(p_0)$, and the minus sign arises because P_I is due to an interference term.

The inverse mean free path (IMFP) is obtained from $P^\sigma(p_0)$ by dividing by $\hbar p_0 / m$. Figure 1 shows the decrease in IMFP which results from including the interference term in Eq. (6) for a variety of electron gas densities as a function of the energy ϵ_{p_0} . This was calculated with use of Eqs. (2), (3), and (6). The sudden drop in the curves represents an increase in the direct-scattering rate due to the onset of plasmon excitation.

The free-electron metal is unpolarized so that

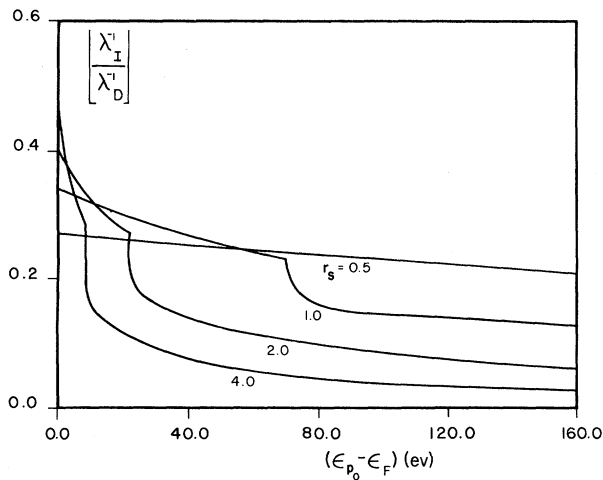


FIG. 1. Calculated interference of direct and exchange IMFP relative to direct IMFP for free-electron gases as a function of incident electron energy. The electron gas interparticle distance r_s is related to the density by $(r_s a_0)^3 = 3/4\pi n$.

$\lambda_{\uparrow}^{-1} = \lambda_{\downarrow}^{-1}$. To relate the free-electron results to ferromagnetic metals, we apply the statistical model and use the density-functional calculations of Moruzzi, Janak, and Williams¹¹ for the charge densities of majority and minority spins in Fe, Co, and Ni. The IMFP's were calculated by averaging over the paramagnetic state of the metal since the spin dependence of the IMFP's is a second-order effect. To calculate the difference in IMFP's, we expand the free-electron IMFP about the paramagnetic state. The difference between parallel and antiparallel IMFP is given by $-\left[\partial\lambda_I^{-1}(n_p)/\partial n\right](n_{\uparrow} - n_{\downarrow})$. Here the particle density of the paramagnetic state is given by $n_p = n_{\uparrow} + n_{\downarrow}$. Here only the interference term enters the spin-dependent difference. Note from Fig. 1 that the sign of $\partial\lambda_I^{-1}/\partial n$ depends on incident electron energy. At very high energies the scattering rate increases with the number of scatterers, so that $\partial\lambda_I^{-1}/\partial n > 0$ as expected intuitively. At very low energies, momentum transfers are limited to $q \leq 2k_F$ and the Coulomb potential v_q causes this feature to dominate the scattering rate. Decreasing the density of an electron gas requires a smaller k_F so that the scattering rate increases and $\partial\lambda_I^{-1}/\partial n < 0$. This behavior is well known for the direct term, Eq. (2). Since $n_{\uparrow} - n_{\downarrow}$ is positive over most of the Wigner-Seitz cell, then the asymmetry A is negative at high energies (i.e., $\lambda^{\uparrow} > \lambda^{\downarrow}$) and positive at low energies (i.e., $\lambda^{\downarrow} > \lambda^{\uparrow}$). This is shown for Fe, Co, and Ni in Fig. 2. For

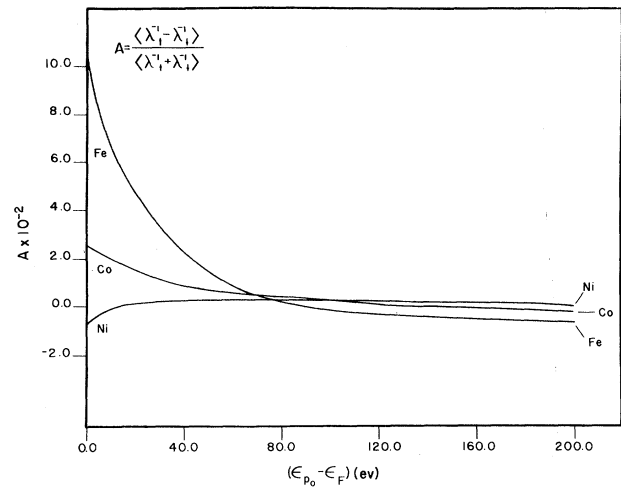


FIG. 2. Calculated difference of IMFP for incident electron with spin parallel and antiparallel to majority spins of Fe, Co, and Ni as a function of incident electron energy.

the case of Ni, the presence of the s and p bands causes a predominance of minority-spin density close to the outer portion of the Wigner-Seitz cell,¹¹ so that at very low energies A changes sign a second time. However, this negative value of A at the Fermi energy in Ni may be an artifact of the statistical approach since electrons in all bands are treated in the same way by this method. The first sign change in A as the incident energy

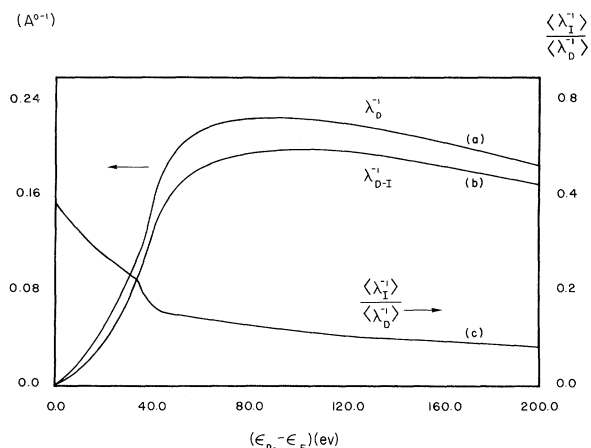


FIG. 3. Curve a , calculated IMFP neglecting exchange scattering; curve b , calculated IMFP including exchange scattering; and curve c , calculated interference of direct and exchange IMFP relative to direct IMFP as a function of incident electron energy. The curves are representative of Fe, Co, and Ni.

decreases is expected to be a general feature which would remain in any improved calculation.

Figure 3 shows plots of the IMFP's both with and without the effect of exchange scattering, and the change in the IMFP due to exchange. The curves for Fe, Co, and Ni all lie within about 4% of each other and we display one representative set of curves. The exchange interference term remains about a 10% effect out to 200 eV above the Fermi energy. This occurs because, although the statistical method gives highest weight to the outer region of the Wigner-Seitz cell where electron densities are lowest, the density of this region corresponds in Fe, Co, and Ni to free-electron gases with $1.0 \leq r_s \leq 1.7$, where $(r_s a_0)^3 = 3/4\pi n(r)$.

¹R. E. DeWames and L. A. Vredevoe, Phys. Rev. Lett. **23**, 123 (1969).

²A. Bringer, M. Campagna, R. Feder, W. Gudat, E. Kisker, and E. Kuhlmann, Phys. Rev. Lett. **42**, 1705 (1979).

³R. Feder, Solid State Commun. **31**, 821 (1979).

⁴M. Campagna, private communication.

⁵R. J. Celotta, D. T. Pierce, G. C. Wang, G. D. Bader, and G. P. Felcher, Phys. Rev. Lett. **43**, 728 (1979).

⁶J. Lindhard and M. Scharff, K. Dan. Vidensk. Selsk., Mat.-Fys. Medd. **27**, No. 15 (1953); J. Lindhard, M. Scharff, and H. E. Schiff, K. Dan. Vidensk. Selsk., Mat.-Fys. Medd. **33**, No. 14 (1963).

⁷C. J. Tung, J. C. Ashley, and R. H. Ritchie, Surf. Sci. **81**, 409 (1979).

⁸R. H. Ritchie and J. C. Ashley, J. Phys. Chem. Solids **26**, 1689 (1965).

⁹J. Lindhard, K. Dan. Vidensk. Selsk., Mat.-Fys. Medd. **28**, No. 8 (1954).

¹⁰J. J. Quinn and R. A. Ferrell, Phys. Rev. **112**, 812 (1958).

¹¹V. L. Moruzzi, J. F. Janak, and A. R. Williams, *Calculated Electronic Properties of Metals* (Pergamon, New York, 1978).

Oscillatory Magnetic Fluctuations near the Superconductor-to-Ferromagnet Transition in ErRh_4B_4

D. E. Moncton, D. B. McWhan, and P. H. Schmidt
Bell Laboratories, Murray Hill, New Jersey 07974

and

G. Shirane and W. Thomlinson
Brookhaven National Laboratory, Upton, New York 11973

and

M. B. Maple, H. B. MacKay, L. D. Woolf, Z. Fisk, and D. C. Johnston
Institute for Pure and Applied Physical Sciences, University of California, San Diego, La Jolla, California 92093
(Received 26 June 1980)

Small-angle neutron experiments show that near the transition from superconductor to ferromagnet in ErRh_4B_4 scattering peaks occur at a wave vector $|\vec{q}_s| = 0.06 \text{ \AA}^{-1}$. The temperature and wave-vector dependence suggest this signal is due to oscillatory magnetization fluctuations caused by the electromagnetic coupling of magnetic and superconducting order parameters. The ferromagnetic Bragg scattering shows a 5% hysteresis and transition-temperature-smearing effects which are also due to magnetic-superconducting interactions.

PACS numbers: 74.70.Lp, 75.25.+z

Superconductivity can develop in systems with large concentrations of magnetic ions if there is a weak interaction between the magnetic moments and the superconducting electrons. Furthermore, if the magnetic ions occupy an ordered lattice as in the rare-earth (RE) ternary superconductors $M\text{Mo}_6X_8$ ($M = \text{Re}; X = \text{S, Se}$) (Ref. 1) and $M\text{Rh}_4\text{B}_4$ (Ref. 2) magnetic order may occur.³ For antifer-

romagnetic order, superconductivity can be preserved. However, in the two known ferromagnetic superconductors, ErRh_4B_4 (Ref. 4) and HoMo_6S_8 (Ref. 5), the materials lose their superconductivity at a second lower-temperature transition.^{6,7} To better understand the interaction between superconducting and magnetic order, we undertook new neutron scattering measurements on ErRh_4B_4